Dispersion properties, birefringence and confinement loss of rotational elliptic air-hole photonic crystal fiber

Tzong-Jer Yang · Yuan-Fong Chau · Han-Hsuan Yeh · Zheng-Hong Jiang · Yao-Wei Huang · Kuang-Yu Yang · Din Ping Tsai

Abstract Dispersion properties, birefringence and confinement loss between the circular air-hole photonic crystal fiber (CAHPCF) and rotational elliptical air-hole photonic crystal fiber (REAHPCF) are investigated numerically by means of a plane-wave expansion method and a finite element method. Results show that the performances of REAHPCF on flatter dispersion curve, single mode, high birefringence and low confinement loss is better than that of CAHPCF.

1 Introduction

Photonic crystal fibers (PCFs) have drawn a great deal of attention from fiber researchers owing to its wide range of unique optical properties that cannot be realized by using conventional fibers [1]. Together with the technological advancement in the fabrication [2, 3] of PCFs, powerful numerical methods [4–7] have been developed to model the guidance properties. Among these above methods, the plane-wave expansion method (PWM) and finite difference method (FEM) are the simpler methods and are able to calculate the mode field distribution, birefringence and confinement loss of the PCFs. By manipulating circular air-hole diameter and pitch Λ (center to center distance between the holes), it is possible to control the PCF dispersion properties. Furthermore, the circular air holes can be replaced by the elliptic ones, in order to obtain more flattened dispersion curve.

To our knowledge, the dispersion curve of rotational elliptical air-hole PCF (REAHPCF) has never been reported. In this paper, we focus on the change of dispersion curve by replacing the circular air holes (CAHs) with elliptic air holes (EAHs), as shown in Fig. 1(a). PWM is used to analyze the dispersion properties. High index core PCF with the zero-dispersion wavelength over a wide range of wavelength has been thus designed. In addition, a comparative study between circular air-hole PCF (CAHPCF) and REAHPCF on birefringence and confinement loss is simulated by FEM.

2 Simulation models, results and discussions

The structure of the PCF used in this study is shown in Fig. 1(a) which is constructed of silica (SiO_2) with a refractive index of $n = 1.492$. As depicted in Fig. 1, elliptical air-hole PCF (EAHPCF) with triangular lattice is design with holes pitch Λ, width of ellipse a, height of ellipse b. The effective index of the fundamental space filling mode (FSM), i.e., the propagation constant of the cladding area, is given by $n_{\text{eff}} = \beta_{\text{FSM}}/k_0$, where β_{FSM} is the propagation constant of the FSM, $k_0 = 2\pi/\lambda$ is the free space wave number. Once the modal effect indices n_{eff} are solved, the dispersion parameter can be obtained. Basically, the waveguide dispersion is strongly related to the design parameters of the PCFs and therefore can be optimized to achieve desired dispersion properties. To verify the suitable value of ellipticity (a/b), Fig. 1(b) depicts the effective index of FSM as a

T.-J. Yang
Department of Electrical Engineering, Chung Hua University, Hsinchu 300, Taiwan, ROC

Y.-F. Chau (✉) · H.-H. Yeh · Z.-H. Jiang
Department of Electronic Engineering, Ching Yun University, Jung-Li 320, Taiwan, ROC
e-mail: yfc01@cyu.edu.tw
Fax: +886-3-3411116

Y.-W. Huang · K.-Y. Yang · D.P. Tsai
Graduate Institute of Applied Physics, National Taiwan University, Taipei, Taiwan, ROC

Fig. 1 (**a**) Cross sectional plane of elliptic air-hole photonic crystal with triangular lattice. (**b**) Effective index of FSM as a function of wavelengths for different a/b value with fixed parameters: $\Lambda = 2.3$ µm and $a = 0.3\Lambda$, respectively

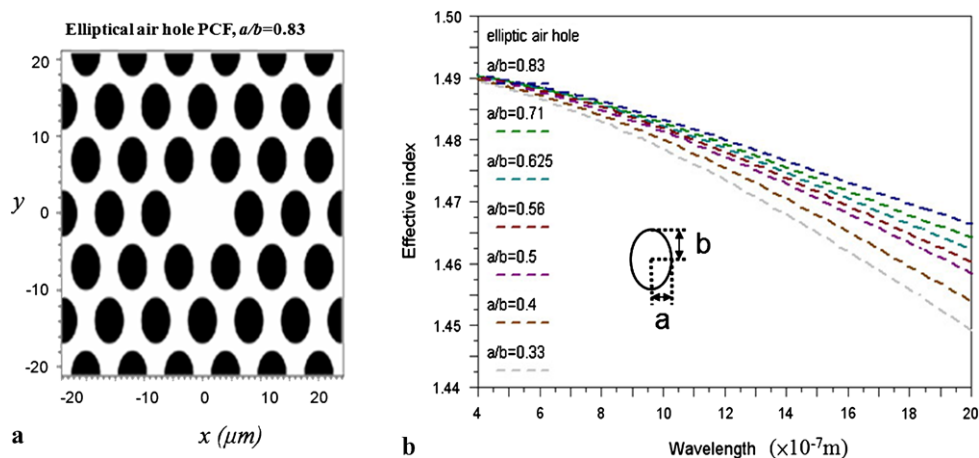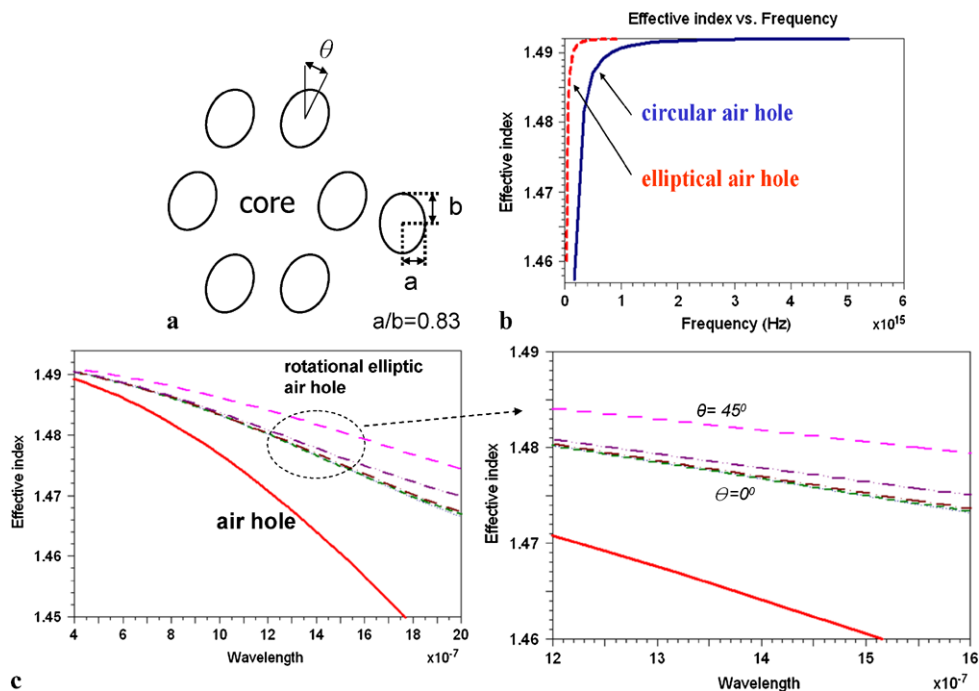**Fig. 2** (**a**) Schematic of REAPCF with rotational angle θ. (**b**) Effective index as a function of frequency between CAPCF (*solid line*) and elliptical air-hole PCF (*dashed line*). (**c**) Effective index as a function of wavelength between CAPCF (*solid line*) and REAPCF (*dashed line*)

function of wavelengths for different a/b with fixed parameters: $\Lambda = 2.3$ µm and $a = 0.3\Lambda$. As can be seen from this figure, higher a/b results in flatter dispersion curve. This is attributed to the higher index difference between short axis and major axis, e.g. $a/b = 0.83$ is larger than that of other a/b in this case. Thus, we use $a/b = 0.83$ throughout this paper if specified otherwise.

Figure 2(b) shows the relation between effective index of FSM and frequency for CAHPCF ($a = b = 0.3\Lambda$) and EAHPCF ($a/b = 0.83$, $\Lambda = 2.3$ µm and $a = 0.3\Lambda$), respectively. It shows that the effective index curve flattens with the increase of frequency and one finds that the EAHPCF reaches steady state at lower frequency. It can be evidenced that EAHPCF has a better dispersion characteristic than the CAHPCF. Figure 2(c) also shows the effective index of FSM as a function of wavelengths for CAHPCF and

REAHPCF ($a/b = 0.83$, θ: $0° \sim 45°$), respectively. Discrepancy of CAHPCF and REAHPCF is strongest for highest θ, as expected, and higher rotational angle θ exhibits a flatter performance on dispersion curve than other cases as shown in Fig. 2(c).

In a conventional step-index fiber, the number of bound modes is governed by the V number ($V = \frac{2\pi a}{\lambda}\sqrt{n_{co}^2 - n_{clad}^2}$, where a is the radius of fiber core, and n_{co} and n_{clad} are the effective index of core and cladding, respectively), which increases without limit as the wavelength decreases. In PCFs, similar results can be defined as $V = \frac{2\pi\Lambda}{\lambda}\sqrt{n_o^2 - n_{eff}^2}$ (where Λ is the air-hole pitch, n_0 is the silica index and n_{eff} is an effective cladding index of FSM). The effective cladding index can be considered as the effective index of the first radiation state, which is equivalent to finding the lowest mode in

the band structure of the plain lattice. It is shown in Ref. [1] that in contrast to step-index fibers, the V_{eff} for a PCF converges to a finite value as the wavelength decreases. If the finite value is less than approximately 2.405, the PCF is single mode. The stationary V_{eff} number is defined by the ratio of a/Λ, and increases with the ratio. Thus by designing a REAHPCF with a/Λ below a certain value, V_{eff} number may be kept under the second-order mode cutoff value over any wavelength range, thereby ensuring an endlessly single-mode operation. For a conventional step-index fiber this cutoff V number is 2.405, and although a different value is expected for the PCF, a cutoff V_{eff} can be approximately 2.5 has been experimentally obtained.

We will evaluate V_{eff} for a range of wavelengths, hole-sizes and θ (varied from 0° to 40°). To find n_{eff}, we only need to simulate one unit cell of the elliptic fiber lattice, and solve for the zeroth eigenvalue. In our case, we change the value of θ with fixing parameters: $\Lambda = 2.3$ μm, $a/b =$ 0.83, $a/\Lambda = 0.3$. Figure 3 shows the variation of V_{eff} with $\log_{10}(\Lambda/\lambda)$ for various θ. The horizontal line corresponds to the single-mode condition, $V_{eff} = 2.405$, the cutoff V value for a step-index fiber. It can be seen from Fig. 3 that higher θ possesses a better performance on single-mode than other case as shown in Fig. 3. Figure 4 shows the variation of V_{eff} as a function of $\log_{10}(\Lambda/\lambda)$ for various a/Λ with fixing parameters: $\Lambda = 2.3$ μm, $a/b = 0.83$ and $\theta = 30°$. It can be clearly seen that lower a/Λ ratio ($a/\Lambda < 0.3$) results in single-mode operation at all wavelengths. In addition, larger holes make the fiber likely to be multimoded. The gaps between the holes become narrower, isolating the core more strongly from silica in the cladding. Smaller holes make single-mode guidance more likely, but the decrease in effective index difference makes the fiber susceptible to bend loss.
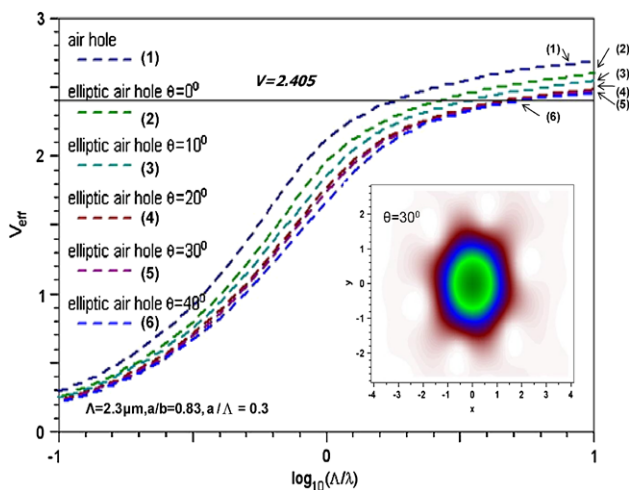
Having analyzed the dispersion properties in the cladding, we turn to the direct calculation of birefringence and confinement loss in REAPCF. The mode index is difficult to be analyzed by PWM due to the large super-cell needed at long wavelength, so we use FEM. It has been confirmed that a perfect triangular lattices PCF with circular symmetric air hole in the cladding does not have birefringence [4], and the fundamental mode of the fiber consists of two degenerate modes. PCF can potentially be made high birefringence: large contrast facilitates high birefringence, and the fabricating techniques permit the versatile arrangement of air holes. In Fig. 2(a), birefringence is introduced by the difference between two orthogonal directions. The doublet components of the fundamental mode, as we know, are degenerate in conventional standard fibers and in CAHPCF with triangular lattice. However, when the air holes are elliptical, the degeneracy splits significantly. Regardless of whether both modes are confined or leaky, the birefringence will be defined as $\Delta n = |n_{eff}^x - n_{eff}^y|$, where n_{eff}^x and n_{eff}^y are the refractive indices of the x- and y-polarization modes, respectively. The effective index and birefringence of PCFs are relative to the varying a/Λ. As expected, the difference between two polarized direction modes in cladding asymmetry can cause high birefringence in PCFs. Figure 5 depicts the birefringence of REHAPCF as function of a/Λ ranging from $a/\Lambda = 0.1$ to 0.5, whereas $a/b = 0.83$ remains constant at excitation wavelength $\lambda = 1.55$ μm. As can be seen from Fig. 5 that the birefringence is sensitive to the varying a/Λ, and the birefringence of REHAPCF is higher than that of non-rotational one. Birefringence will increase to a level above 0.001 as shown in Fig. 5, the family curves of birefringence shift upward, corresponding to an increase in the a/Λ value. It may then be concluded that rotating the angle of elliptical air holes in PCF cladding increases the birefringence. The increment is much more significantly at higher a/Λ than that of shorter one. With the appropriate
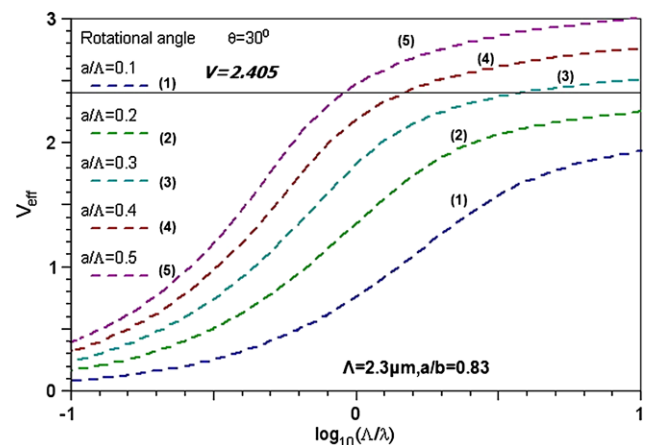

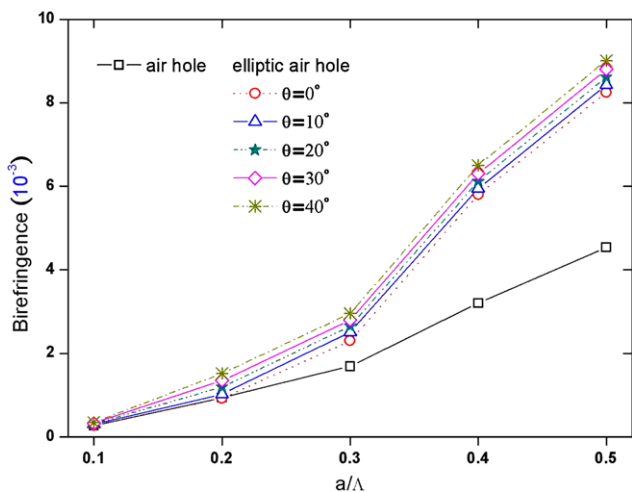**Fig. 3** Variation of V_{eff} with $\log_{10}(\Lambda/\lambda)$ for various rotational θ. *Insets*: distribution of H_x in fundamental mode of REAPCF with $\theta = 30°$.

Fig. 4 Variation of V_{eff} with $\log_{10}(\Lambda/\lambda)$ for various relative ratio a/Λ

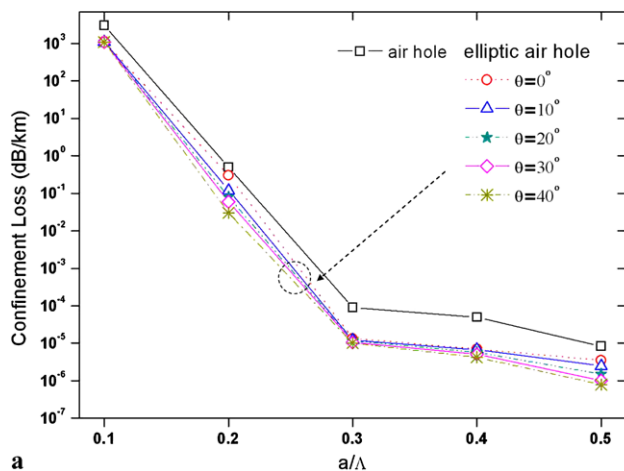**Fig. 5** Birefringence as a function of a/Λ for various θ

rotational angle of elliptical air hole ranging from $\theta = 15°$ to 40°, higher birefringence may be achieved.

FEM with perfectly matched layers, which are placed before the outer boundary can be used to calculate the confinement loss of PCFs. The imaginary part of complex effective index represents the loss. For small holes and few holes rings, the confinement loss is huge, but decreases rapidly as air-hole diameter increases or more air-hole rings are employed [8, 9]. Figure 6(a) shows the confinement loss as a function of a/Λ at different rotational angles of elliptical air holes with the fixed parameters: $\lambda = 1.55$ μm, $a/b = 0.83$, number of air-hole rings $N = 7$. It can be observed that the confinement loss at different θ is less than 10^{-5} dB/km when the $a/\Lambda \leq 0.3$. This shows that the effect of REAPCF cladding on the optical loss is small, and can be achieved one order of magnitude smaller than that of CAHPCF.

Figure 6(b) also shows the confinement loss as a function of wavelength at different rotational angles of elliptical air holes with the fixed parameters: $a/b = 0.83$, $N = 7$ and $a/\Lambda = 0.3$. It can be seen in Fig. 6(b) that the confinement loss for rotational case is in the range of $1.02 \times 10^{-5} \sim 5.35 \times 10^{-5}$ dB/km and for circular air-hole case is 5.3×10^{-3} dB/km at excitation wavelength $\lambda = 1.55$ μm. If the PCF is required to have an acceptable confinement loss ≤ 0.1 dB/km, the birefringence will increase to a level above 0.001. Thus, there is a tradeoff between the confinement loss and the birefringence for a rotational elliptical-hole with triangular lattice PCF like a structure of Fig. 2(a) which indicating that the high mode birefringence and low confinement loss are maintained.

3 Conclusion

In conclusion, dispersion properties, birefringence and confinement loss between the CAPCF and REAHPCF are investigated numerically by means of PWM and FEM. Results
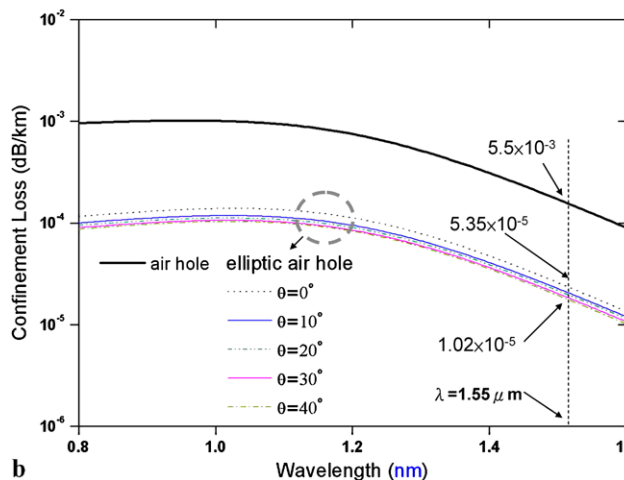
Fig. 6 (**a**) Confinement loss as a function of (**a**) a/Λ and (**b**) wavelength for various θ

show that the performance of REAHPCF on flatter dispersion curve, single mode, high birefringence and low confinement loss is better than that of CAHPCF. As an example, how to design the structure parameters for engineering the chromatic dispersion, higher birefringence and low confinement loss of REAHPCF is designed and demonstrated. The suggested REAHPCF can be fabricated by the stack and draw procedure, which will open new possibilities high performance PCF over the conventional fiber.

References

1. J.C. Night, P.S. Russell, Science **296**, 276 (2002)
2. P. Falkenstein, C.D. Merritt, B.L. Justus, Opt. Lett. **29**, 1858 (2004)
3. T.A. Birks, J.G. Knight, P.S. Russel, Opt. Lett. **22**, 961 (1997)
4. J.D. Joannopoulos, R.D. Meade, J.N. Winn, *Photonic Crystals: Molding the Flow of Light* (Princeton University Press, New York, 1995)

5. A. Cucinotta, S. Selleri, L. Vincetti, M. Zoboli, IEEE Photonics Technol. Lett. **14**, 1530 (2002)
6. Z. Zhu, T.G. Brown, Opt. Express **10**, 853 (2002)
7. F. Fogli, L. Saccomandi, P. Bassi, G. Bellanca, S. Trillo, Opt. Express **10**, 54 (2002)
8. Y.-F. Chau, H.-H. Yeh, D.P. Tsai, Jpn. J. Appl. Phys. **46**, L1048 (2007)
9. Y.-S. Sun, Y.-F. Chau, H.-H. Yeh, T.-J. Yang, D.P. Tsai, Appl. Opt. **46**, 5276 (2007)